

Chapter 27

Shelf sea modelling

27.1 Test case *bohai*

The aim of this test case is to illustrate the use of COHERENS for tidal prediction studies, to show how an harmonic analysis can be performed and how an analysis can be made of the distribution, propagation and dissipation of tidal energy. The Bohai Sea is situated in the northern part of the Yellow Sea between the Northeast coast of China and the Korean peninsula. The simulated area is between $117^{\circ}5'E$ – $125^{\circ}35'E$ and 37° – $41^{\circ}5'N$. Water depths, shown in Figure 27.1, are lower than 50 m in the western and between 60–85 m in the central eastern part.

The tides enter the domain through the southern boundary. Two tidal constituents (M_2 and S_2) are imposed in harmonic form, as given by equation (4.354) without the first (residual) term. The grid has an horizontal resolution of $5'$ in longitude and latitude. The time step for the barotropic (2-D) mode is 30 s. The simulations are performed either in depth-averaged mode or using a full 3-D grid. The bottom stress is calculated using the 2-D quadratic law (4.341) in the 2-D and (4.340) in the 3-D case. The bottom drag coefficient is calculated from either (4.343) or (4.344) using a constant roughness length $z_0=0.0035$ m. The baroclinic time step is set to 5 min and 20 uniform σ -levels are taken in the vertical. The simulated period is 16 days, covering a full spring-neap cycle. Results are harmonically analysed for the two tidal constituents. Analysed output consists of the amplitudes and phases of water levels and currents, parameters of tidal ellipses and energy parameters (kinetic and potential energy, energy dissipation and fluxes).

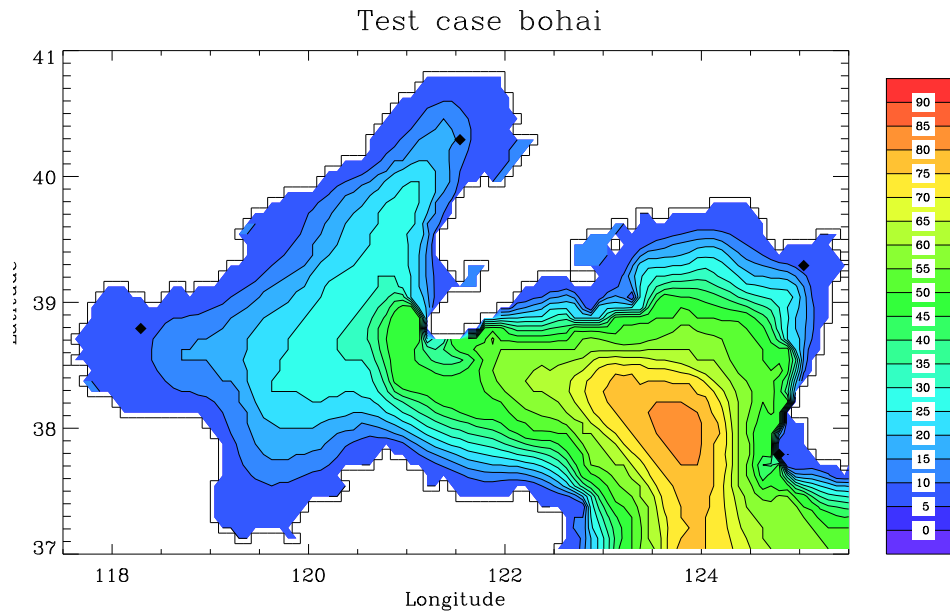


Figure 27.1: Bathymetry of the Bohai Sea. The diamond symbols locate the position of the 4 four stations used in the definition of the output parameters.

27.1.1 Experiments and output parameters

Six experiments are defined in the bohai test case. The aim is to compare three different types of open boundary conditions either in 2-D and 3-D mode.

A : A 2-dimensional grid is taken. At the open boundaries the characteristic method with specified elevation is applied.

B : As experiment **A** now using the Flather condition (4.367) at open boundaries.

C : As experiment **A** now using the local solution (4.360) at open boundaries.

D : As **A** now using a 3-D grid.

E : As **B** now using a 3-D grid.

F : As **C** now using a 3-D grid.

A series of output parameters are defined. The first five are global residuals obtained from the harmonic analysis.

- ekin The domain integrated kinetic energy $\langle \bar{E}_k \rangle$ (in 10^{15} J) with \bar{E}_k defined by (D.8) in the 2-D and (D.11) in the 2-D case.
- epot The domain integrated potential energy $\langle E_p \rangle$ (in 10^{15} J) with E_p defined by (D.3).
- etot The domain integrated total energy (in 10^{15} J) given as the sum of ekin and epot.
- bdissip The domain integrated negative energy dissipation $-\langle \bar{D} \rangle$ with \bar{D} defined by (D.13) in the 2-D or (D.10) in the 3-D case.

The next series of parameters gives the location of the four amphidromic points (two for the M_2 and two for the S_2 tide) which are determined as local minima of ζ .

- zetmin Value of the local minimum for ζ (m).
- xpos Longitude of the amphidromic point (decimal degrees East)
- ypos Latitude of the amphidromic point (decimal degrees North)

The last series of parameters are the amplitudes and phases of the surface elevation, and the elliptic parameters obtained from harmonic analysis for the two tidal constituents at 4 stations.

- M2-zetamp M_2 amplitude of the sea level height (cm)
- M2-zetpha M_2 phase of the sea level height (cm)
- M2-ellmaj major axis of the M_2 tidal ellipse (cm)
- M2-ellipt ellipticity of the M_2 tidal ellipse
- M2-ellinc inclination of the M_2 tidal ellipse (degrees)
- M2-ellpha elliptic phase of the M_2 tidal ellipse (degrees)
- S2-zetamp S_2 amplitude of the sea level height (cm)
- S2-zetpha S_2 phase of the sea level height (cm)
- S2-ellmaj major axis of the S_2 tidal ellipse (cm)
- S2-ellipt ellipticity of the S_2 tidal ellipse
- S2-ellinc inclination of the S_2 tidal ellipse (degrees)
- S2-ellpha elliptic phase of the M_2 tidal ellipse (degrees)

For a definition of the tidal ellipse parameters see Section 4.12.2.

27.1.2 Results

The following figures are produced for experiment **A**.

- Amplitudes and phases of the sea surface elevation, major axis and ellipticity of the tidal ellipse are shown in Figures 27.2 for the M_2 and 27.3 for the S_2 tide.
- Figure 27.4 displays time series of the domain averaged kinetic, potential, total energy and energy dissipation.
- Spatial distributions of the residual depth-mean tidal energy, energy dissipation and tidal energy flux, as defined by equations (D.11), (D.13) and (D.12) are given in Figure 27.5.

The results can be summarised as follows

- Both the M_2 and S_2 tide show the same two amphidromic points located respectively in the Southwest and Southeast parts of the domain. The positions are the same for all experiments.
- From figures 27.2 and 27.3 one infers that the M_2 amplitudes for elevation and currents are 2 to 2.5 times higher than the ones obtained from the S_2 tide. The tides themselves show a strong variability over the domain with much larger amplitudes for elevations and currents (up to a factor 5) in the eastern compared to the western parts. From the distributions of tidal ellipticity one observes rapid changes from nearly circular to rectilinear ellipses and from cyclonic to anticyclonic motions.
- There is no difference between the tests using the open boundary condition with the local solution and the one with the characteristic method and a very small difference with the test using the Flather condition, both for the 2-D as for the 3-D case. Larger differences are seen between the 2-D and 3-D runs. Although these can be still be considered as small for the amplitudes, a phase difference of a few degrees can be observed. Since the tidal flow is mainly barotropic with no shear, except at the bottom (not shown), this can only be explained by the different formulation for the bottom stress.
- The residual and domain-averaged kinetic and potential are nearly the same, in analogy with linear surface waves. The time series of the non-analysed energy parameters exhibits a strong spring-neap cycle since the amplitude ratio equals the square of the ones obtained for elevations and currents.

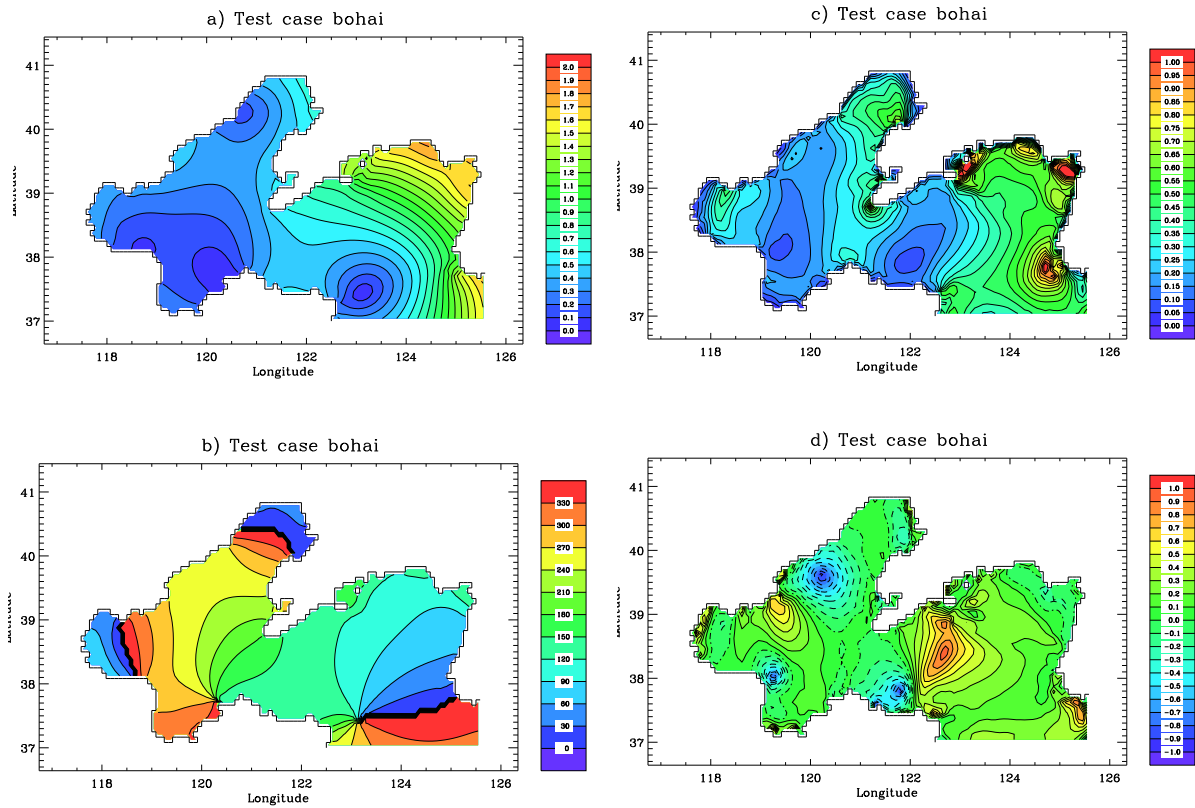


Figure 27.2: Amplitudes in cm (a), phases in degrees (b) of the surface elevation, major axis in m (c) and ellipticity (d) for the M_2 tide and experiment *bohaiA*.

- As expected from the previously discussed tidal distributions, tidal energy is mainly concentrated in the eastern parts. The propagation of tidal energy is mainly concentrated along the slopes of the bathymetry (Figure 27.5c). Energy dissipation only occurs within well-defined coastal areas in the eastern parts.

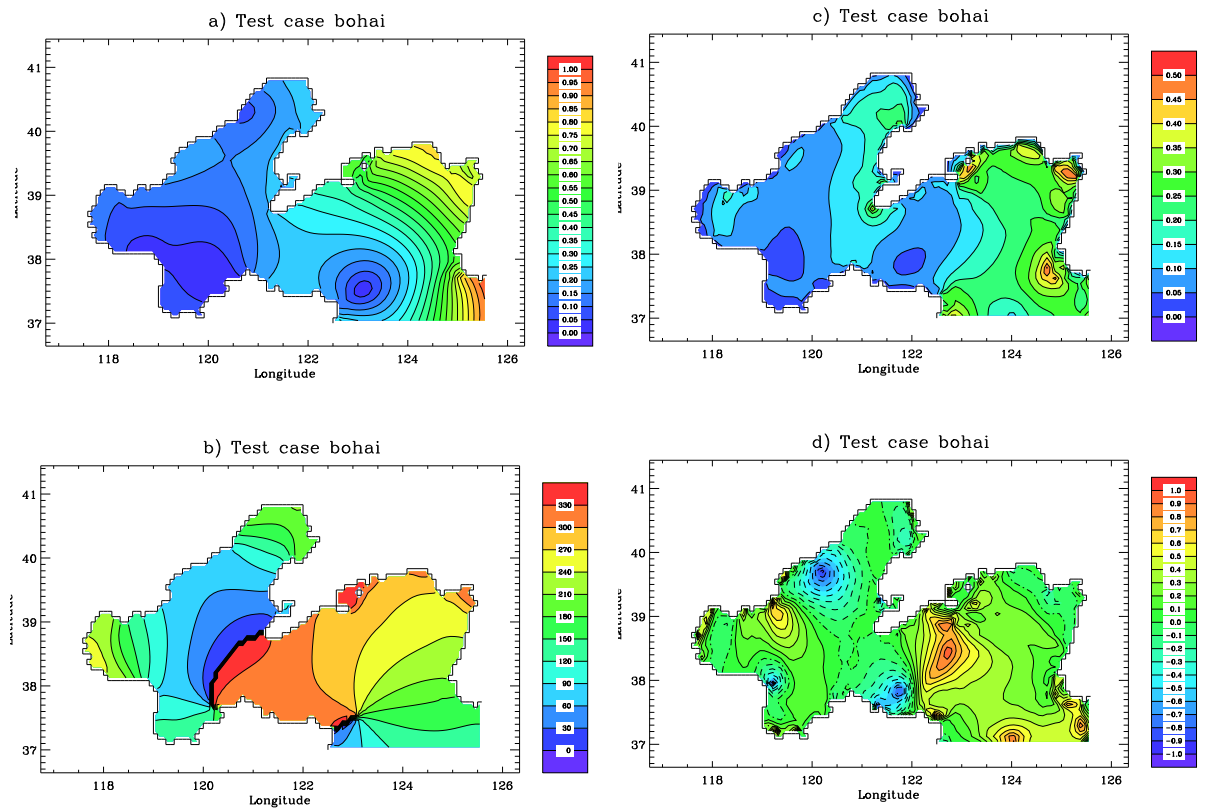


Figure 27.3: Amplitudes in cm (a), phases in degrees (b) of the surface elevation, major axis in m (c) and ellipticity (d) for the S_2 tide and experiment *bohaiA*.

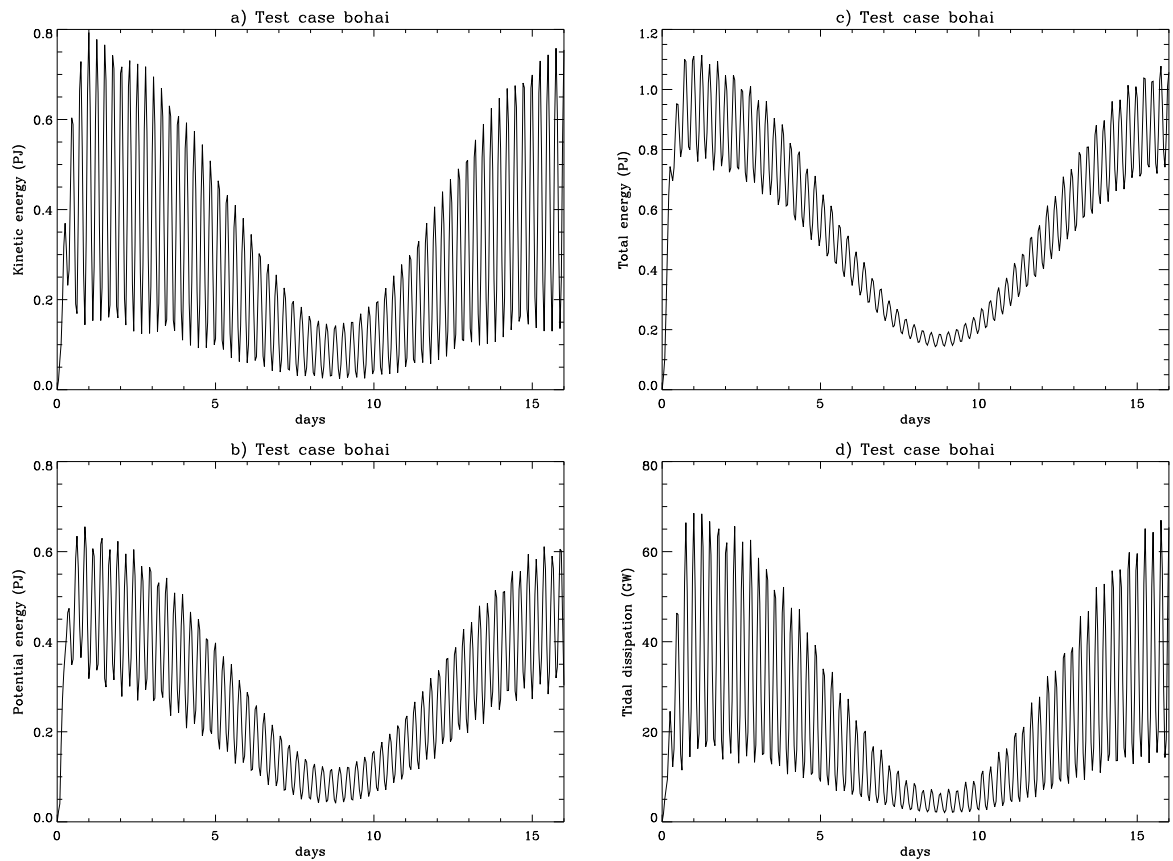


Figure 27.4: Time series of (a) the domain-integrated kinetic energy (10^{15} J), (b) potential energy (10^{15} J), (c) total energy (10^{15} J) and (d) energy dissipation (10^9 W) for experiment *bohaiA*.

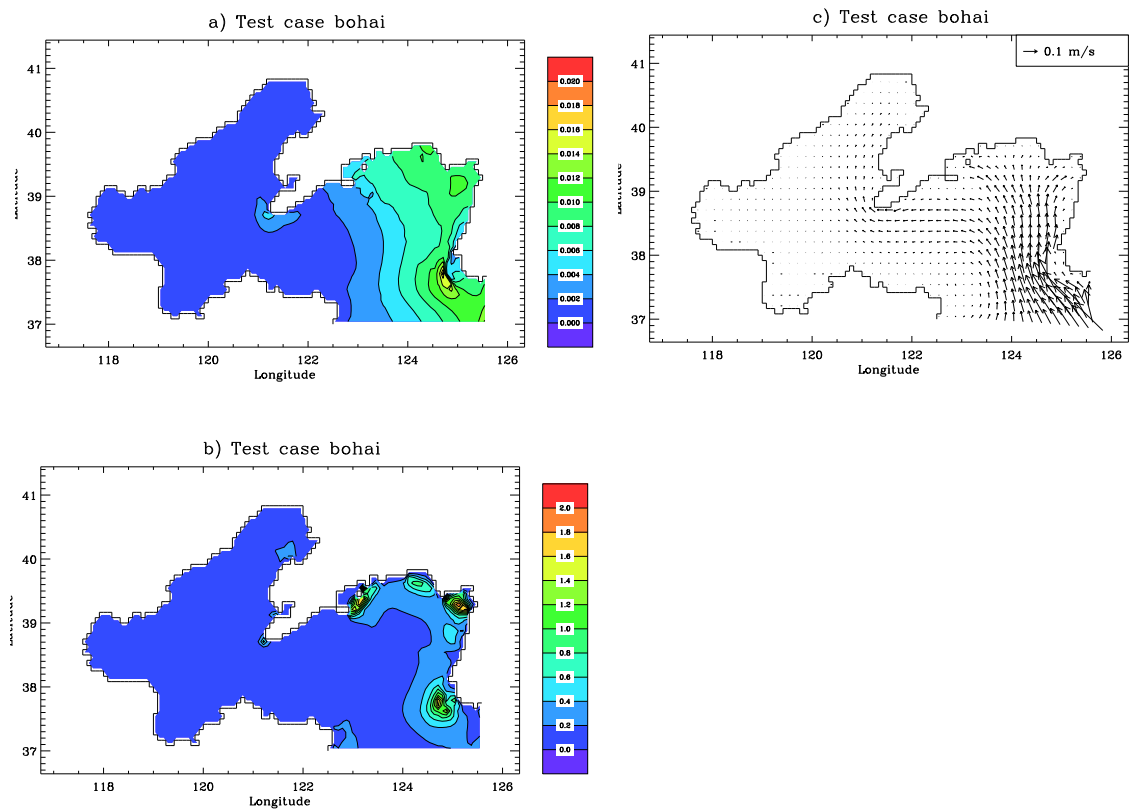


Figure 27.5: Distribution of the depth-integrated residual tidal energy (a), depth-integrated energy dissipation (b) and energy flux (c) for experiment *bohaiA*. Units are 10^6J/m^2 (a), W/m^2 (b), 10^6W/m (c).